

# Neural Network-Based Sequential Global Sensitivity Analysis Algorithm

Yen-Chen Liu<sup>1</sup>[0000-0003-1769-9738], Leifur Leifsson<sup>2</sup>[0000-0001-5134-870X],  
Slawomir Koziel<sup>3,4</sup>[0000-0002-9063-2647], and Anna  
Pietrenko-Dabrowska<sup>4</sup>[0000-0003-2319-6782]

<sup>1</sup> Department of Aerospace Engineering, Iowa State University, Ames IA 50011, USA  
[clarkliu@iastate.edu](mailto:clarkliu@iastate.edu)

<sup>2</sup> School of Aeronautics and Astronautics, Purdue University, West Lafayette, IN  
47907, USA  
[leifur@purdue.edu](mailto:leifur@purdue.edu)

<sup>3</sup> Engineering Optimization & Modeling Center, Department of Engineering,  
Reykjavík University, Menntavegur 1, 102 Reykjavík, Iceland  
[koziel@ru.is](mailto:koziel@ru.is)

<sup>4</sup> Faculty of Electronics Telecommunications and Informatics, Gdansk University of  
Technology, Narutowicza 11/12, 80-233 Gdansk, Poland  
[anna.dabrowska@pg.edu.pl](mailto:anna.dabrowska@pg.edu.pl)

**Abstract.** Performing global sensitivity analysis (GSA) can be challenging due to the combined effect of the high computational cost, but it is also essential for engineering decision making. To reduce this cost, surrogate modeling such as neural networks (NNs) are used to replace the expensive simulation model in the GSA process, which introduces the additional challenge of finding the minimum number of training data samples required to train the NNs accurately. In this work, a recently proposed NN-based GSA algorithm to accurately quantify the sensitivities is improved. The algorithm iterates over the number of samples required to train the NNs and terminates using an outer-loop sensitivity convergence criteria. The iterative surrogate-based GSA yields converged values for the Sobol' indices and, at the same time, alleviates the specification of arbitrary accuracy metrics for the NN-based approximation model. In this paper, the algorithm is improved by enhanced NN modeling, which lead to an overall acceleration of the GSA process. The improved algorithm is tested numerically on problems involving an analytical function with three input parameters, and a simulation-based nondestructive evaluation problem with three input parameters.

**Keywords:** Global sensitivity analysis · surrogate modeling · neural networks · Sobol' indices · termination criteria.

## 1 Introduction

The study of sensitivity analysis (SA) [1, 2] is important in many engineering and science applications. Individual effects and interactions of the input parameters

on the output model response can be quantified by SA [3, 4]. Engineers and scientists can use SA to understand the importance of parameters in experimental or computational investigations. There are two types of SA, local [5] and global [6] SA. Local SA usually refers to using the the local output model response to quantify the effect of small local perturbations in the inputs. In global SA, it utilizes the variance of output model response to quantify the effect due to the input variability in the entire parameter space. This work focuses on the use of global variance-based SA with Sobol’ indices [3, 4] for simulation-based problems.

In this paper, a recently developed algorithm for surrogate-based GSA [7] is improved and applied to new testing problems. In the NN-based sequential algorithm, the number of samples is iteratively increased with the goals of obtaining the converged Sobol’ indices with the training cost as minimum as possible. This approach not only alleviates the needs to specify arbitrary surrogate modeling accuracy metrics, but also reliefs from the fact that accuracy metrics for surrogate models do not guarantee that converged Sobol’ indices are obtained. In this work, the implementation of the NN training has been improved significantly, which leads to improved convergence of the GSA algorithm. The algorithm is tested numerically on two problems; an analytical function with three parameters and a simulation-based problem with five parameters.

The next section describes the problem statement and gives the details of the GSA algorithm. The following section presents results of numerical experiments. Finally, conclusions are presented and remarks on future steps are given.

## 2 Methods

This work proposes a sequential algorithm to quantify the global sensitivities of each input variability parameter to the simulation-based model outputs. Figure 1 shows the flowchart of the proposed algorithm. The algorithm starts from an initial sample plan,  $\mathbf{x}$ , which takes a small number of samples from the input parameters with their variability. Latin hypercube sampling (LHS) [8] is used in this work to randomly select sample data points from each probability distribution of the inputs. The corresponding outputs or observations,  $y$ , are then generated from the simulation model. A surrogate model,  $\hat{y}(\mathbf{x})$ , is constructed using these inputs and outputs as training data. The input-output behavior of the simulation model is imitated by the surrogate. Next, GSA is performed with this surrogate model using Sobol’ sensitivity indices. The calculation of the Sobol’ indices is a Monte Carlo process, therefore the convergence of these indices are checked within an inner-loop. In the inner-loop, the Sobol’ indices are computed by sampling the current surrogate model, and the number of samples is increased during each iteration (e.g., one order of magnitude for this work) until it achieves the convergence of the inner-loop. Then, the converged inner-loop indices are checked by the outer-loop. The above process is resampled with an increasing number of sample plan from the simulation model until the outer-loop convergence criteria are met. The number of sample plan affects training an

accurate surrogate model, and the outputs of the surrogate affect the precision of the GSA. The outcome of the proposed algorithm yields the corresponding surrogate model and the converged Sobol' indices of GSA.

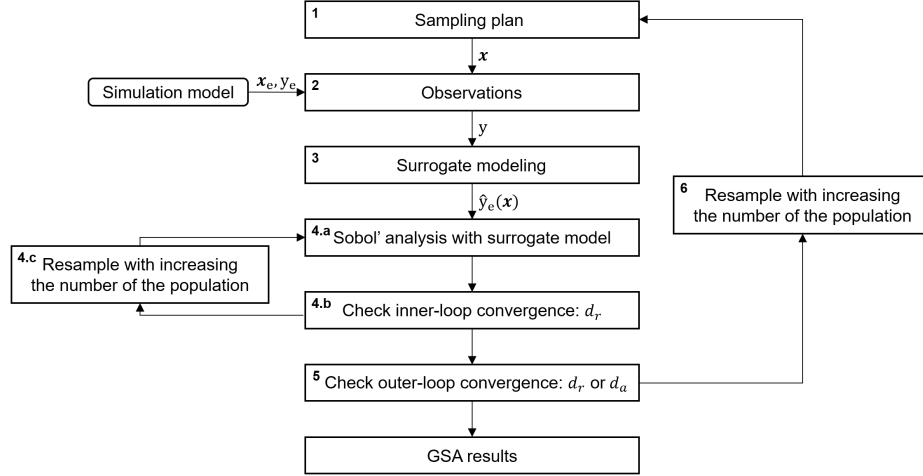


**Fig. 1:** A flowchart of the sequential global sensitivity analysis algorithm with neural network-based prediction.

Neural networks (NNs) are used in a variety of applications in the world. In this work, NN is used to be the surrogate and mimic the behavior of the simulation model. The general structure of NN is a hierarchy of features [9] with three parts: input layer, output layer, and hidden layers [10, 11]. All the layers are composed by "neurons" which are the fundamental units of computation [9]. The number of neurons in the input and output layers are the same as the number of input and output variables of the simulation model. Hidden layers are the layers in-between the input and output layers. There could be zero or more hidden layers in a neural network. The number of hidden layers and the number of neurons in each hidden layer usually varies from case to case.

This work uses Sobol' indices [3, 4] for the global sensitivity analysis. It is a variance-based method that quantifies the single effects of individual inputs and the interactions of combination of inputs on the simulation model output. The first-order Sobol' indices [4] that quantify the effect of individual inputs are given by

$$S_i = \frac{V_i}{\text{Var}(y)} = \frac{\text{Var}_{x_i}(E_{\mathbf{x}_{\sim i}}(y|x_i))}{\text{Var}(y)}, \quad (1)$$

where  $S_i$  is the contribution of individual  $x_i$  on the output variance of the simulation model. The total-order or total-effect Sobol' indices [4] that quantify the

interactions of combined inputs are given by

$$S_{T,i} = 1 - \frac{\text{Var}_{\mathbf{x}\sim i}(E_{x_i}(y|\mathbf{x}\sim i))}{\text{Var}(y)}, \quad (2)$$

where  $S_{T,i}$  measures the contribution of both individual  $x_i$  and the interactions between  $x_i$  and other input parameters on the output variance of the simulation model.

The proposed sequential algorithm includes an outer-loop that samples the simulation model to generate the NN-based surrogate models and an inner-loop that samples the trained NN-based surrogate model to compute the Sobol' sensitivity indices. The converged NN-based surrogate model and Sobol' indices are obtained by the termination of the outer- and inner-loop based on two measurements of the Sobol' indices between successive iterations. The first measurement is computed by the absolute relative change of Sobol' indices defined as

$$d_r[s_i] = \left| \frac{s_i^{(n)} - s_i^{(n-1)}}{s_i^{(1)}} \right|, \quad (3)$$

where  $s$  is the value of the Sobol' indices and is calculated separately for first- and total-order indices,  $i$  is the index of input parameter, and  $n$  is the current iteration index. The loop is terminated when  $d_r[s_i] \leq \epsilon_r$  for all  $s_i$ . In this work,  $\epsilon_r$  is set to 0.1. The second measurement is computed by the absolute change of Sobol' indices, given by

$$d_a[s_i] = \left| s_i^{(n)} - s_i^{(n-1)} \right|, \quad (4)$$

where  $s$  is the value of the Sobol' indices and is calculated separately for first- and total-order indices,  $i$  is the index of input parameter, and  $n$  is the current iteration index. The loop is terminated when  $d_a[s_i] \leq \epsilon_a$  for all  $s_i$ . In this work,  $\epsilon_a$  is set to 0.01. Both outer- and inner-loop can be terminated by either  $d_r[s_i] \leq \epsilon_r$  or  $d_a[s_i] \leq \epsilon_a$  being true.

### 3 Numerical Experiments

#### 3.1 Case 1: Analytical function

An analytical function with three input variables and one single output function is used to demonstrate the algorithm. The function is written as

$$f(\mathbf{x}) = x_1 + x_2 x_3^2, \quad (5)$$

where  $x_1 \in U(0, 1000)$ ,  $x_2 \in U(0, 100)$ , and  $x_3 \in U(0, 10)$  are the input parameters and their associated PDFs, and  $y$  is the function output.

Figure 2 shows the convergence of the direct GSA of the true model. Direct GSA converged at 1000 sampling points. Figure 3 shows the inner-loop GSA

convergence using the NN-based algorithm and Fig. 4 shows the outer-loop convergence. The algorithm terminates at 200 samples. The NN models are trained using two hidden layers, with twenty neurons, and the tangent hyperbolic activation function. The learning rate is set to 0.001 and the batch size is set to 16. The maximum number of epochs and  $\beta_1$  are set to 2,000 and 0.9, respectively. L2 regularization is used with  $\lambda=0.1$  while training the models.

Table 1 shows a comparison of the global sensitivities obtained from direct and NN-based numerical experiments. It can be seen that the NN-based yields global sensitivities within 1.7% of the true values while using only a fraction of the cost of the direct approach.

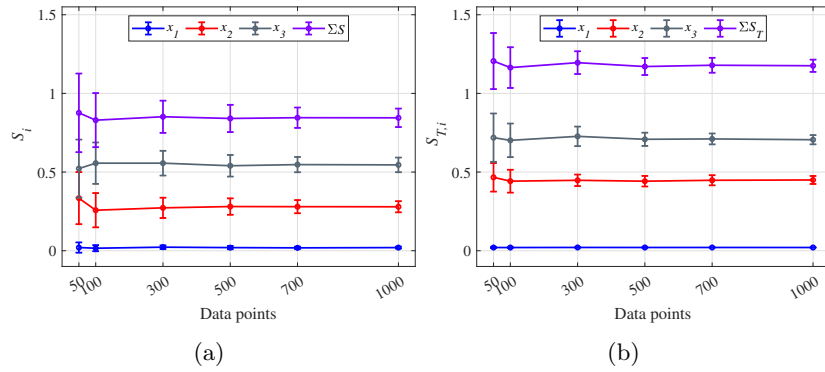


**Fig. 2:** Case 1 convergence of GSA directly on the true model: (a) first-order indices, and (b) total-order indices.

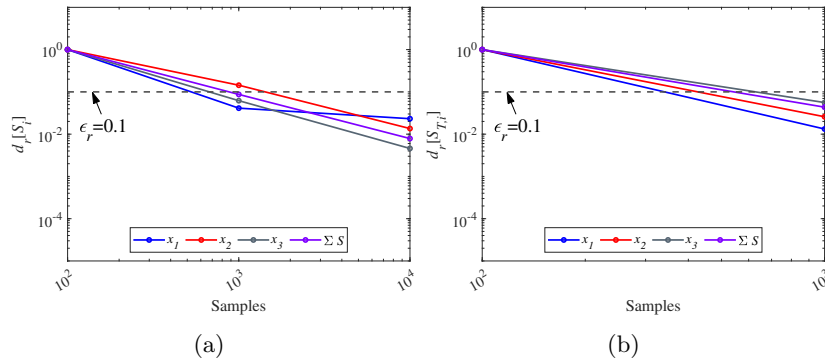


**Fig. 3:** Case 1 inner-loop convergence of  $s_i$  for the NN trained with 100 LHS samples: (a) first-order indices, and (b) total-order indices.

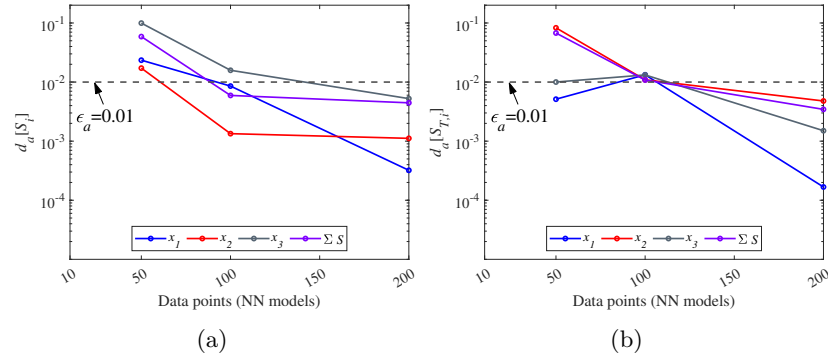


**Fig. 4:** Case 1 outer-loop convergence of  $s_i$  terminated on  $d_a \leq \epsilon_a$  criteria: (a) first-order indices, and (b) total-order indices.

**Table 1:** Case 1 comparison of Sobol' index values between the true model and the converged NN model.

$\mathbf{x}$	$S_i$			$S'_{T,i}$		
	True function	Seq. GSA	% error	True function	Seq. GSA	% error
$x_1$	0.0199	0.0201	1%	0.0204	0.0201	1.5%
$x_2$	0.2793	0.2745	1.7%	0.4497	0.4453	1%
$x_3$	0.5456	0.5347	2%	0.7065	0.7053	0.2%

### 3.2 Case 2: Ultrasonic testing (UT) of a pillbox-defect

In this numerical experiment the pillbox-inclusion-defect under planar transducer ultrasonic (UT) nondestructive testing (NDT) benchmark case is used [12, 13]. Figure 5 shows the setup of the problem. The planar transducer is placed in water and the probe angle ( $\theta$ ) and the probe coordinates ( $x$  and  $y$ ) are varied. A fused quartz block with a pillbox-like void is inspected by the transducer where the distance between the transducer and the surface of the block ( $z_1$ ) and the distance between the surface of the block and the defect ( $z_2$ ) can vary based on the setup. The variability parameters with their associated PDFs are  $\theta \in N(0, 0.5^2)$  deg,  $x \in U(0, 1)$  mm,  $y \in U(0, 1)$  mm,  $z_1 \in U(24.9, 25.9)$  mm, and  $z_2 \in U(12.5, 13.5)$  mm. The output response is the reflected pulse ( $v$ ) received by the transducer.

The simulation model for this case uses the Kirchhoff approximation (KA) to simulate the voltage wave receives by the transducer. The center frequency of the planar transducer is set to 10 MHz. The longitudinal wave speed is set to 6,200 m/s, and the shear wave speed is set to 3,180 m/s. The density of the fused quartz block is set to 4,420 kg/m<sup>3</sup>. The NN models in this case are trained using two hidden layers, with thirty neurons. Similar to the previous case, the tangent hyperbolic activation function is used. The learning rate and  $\beta_1$  of the

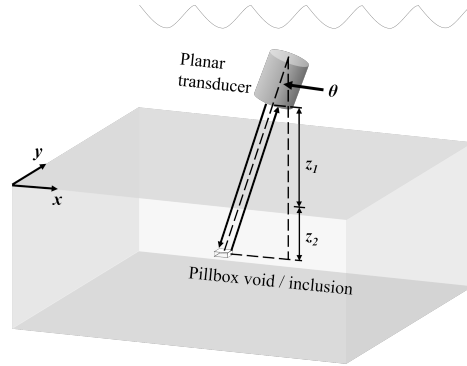


**Fig. 5:** A schematic of setup for the ultrasonic testing case.

ADAM optimizer are set to 0.001 and 0.9, respectively. The batch size is set to 16 and the maximum number of epochs is set to 2,000. L2 regularization is used with  $\lambda=0.1$  while training the models.

Figure 6 shows the direct GSA converged at 3000 sampling points. The convergence criteria of sequential GSA in this case were the same as in the previous case. The outer-loop sequentially iterated from 100 to 400 LHS samples. Figures 7(a) and 7(b) show the inner-loop GSA convergence using the NN-based algorithm for the first- and total-order indices require  $10^6$  and  $10^3$  samples, respectively. Figure 8 shows the outer-loop convergence plots for the first- and total-order indices both terminated at 400 samples. Figure 9 shows that the distance from the transducer to the defect has a negligible effect on the output response, while the probe angle has the highest effect follows by  $y$  coordinate then  $x$  coordinate. Table 2 compares the Sobol' indices values from the proposed method to those from the true function. It shows a good match of the the Sobol' indices values while the cost of sequential GSA is an order of magnitude less than the direct GSA.

**Table 2:** Case 2 comparison of Sobol' index values between the true model and the converged NN model.

$\mathbf{x}$	$S_i$			$S_{T,i}$		
	true model	Seq. GSA	% error	true model	Seq. GSA	% error
$\theta$	0.5599	0.56	0.02%	0.7424	0.7456	0.4%
$x$	0.0623	0.0571	8.3%	0.2086	0.2082	0.2%
$y$	0.1841	0.1919	4.2%	0.2449	0.2467	0.7%
$z_1$	$5.2 \times 10^{-5}$	$6.5 \times 10^{-5}$	-	$5.3 \times 10^{-5}$	$1.0 \times 10^{-4}$	-
$z_2$	$6.6 \times 10^{-4}$	$5.2 \times 10^{-4}$	-	$8.4 \times 10^{-4}$	$7.6 \times 10^{-4}$	-

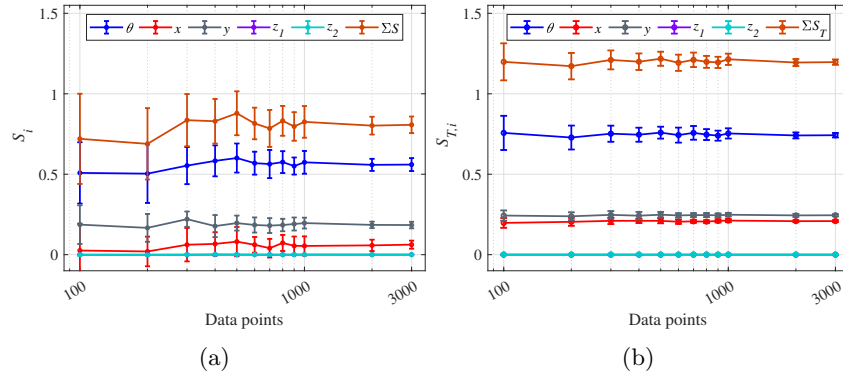


**Fig. 6:** Case 2 convergence of GSA directly on the physics model: (a) first-order indices, and (b) total-order indices.

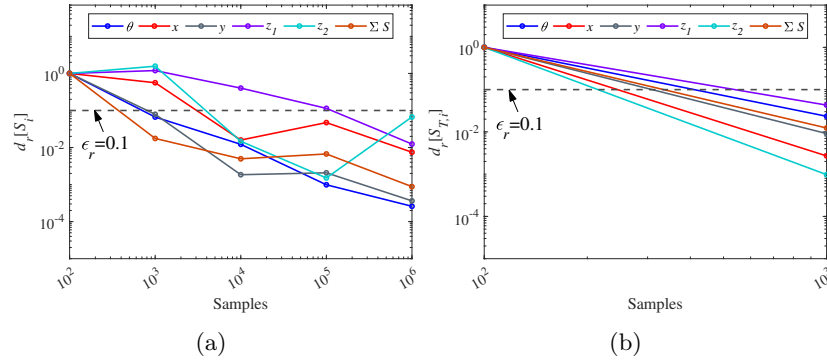


**Fig. 7:** Case 2 inner-loop convergence of  $s_i$  for the NN trained with 400 LHS samples: (a) first-order indices, and (b) total-order indices.

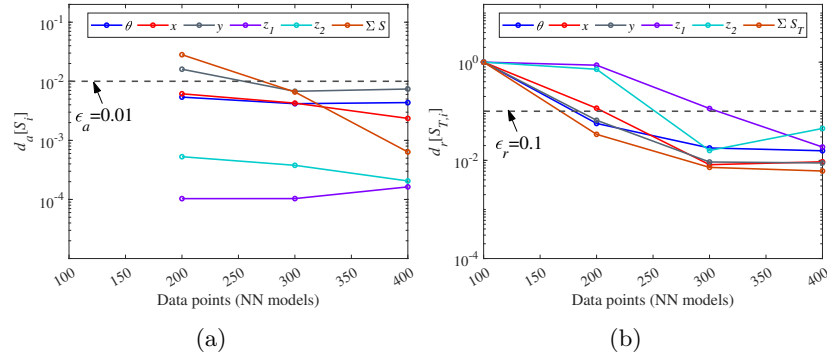


**Fig. 8:** Case 2 outer-loop convergence of  $s_i$  terminated on (a)  $d_a \leq \epsilon_a$  criteria: first-order indices, and on (b)  $d_r \leq \epsilon_r$  criteria: total-order indices.



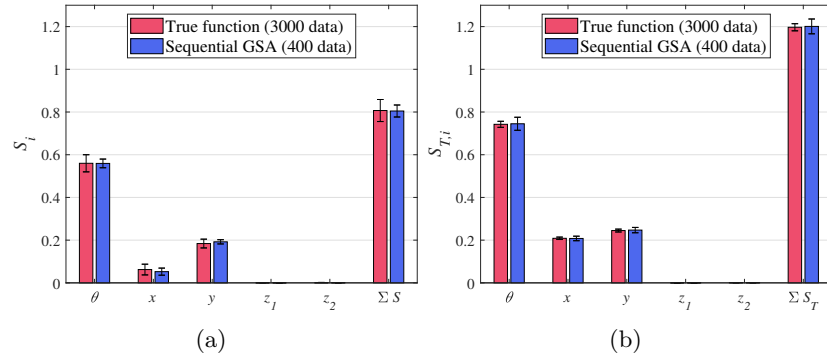


**Fig. 9:** Case 2 Sobol' index values of input parameters computed by the converged NN model: (a) first-order indices, and (b) total-order indices.

## 4 Conclusion

Global sensitivity analysis (GSA) of large-scale data sets is an important problem in engineering and science decision-making. The algorithm presented in this paper directly tackles this important task in the context of simulation-based problems. In particular, this work demonstrates that simulation-based GSA using neural network-based function prediction can be iteratively improved and terminated once accurate sensitivities are obtained, thereby enabling efficient adaptive GSA for large-scale problems.

Future steps in this work will focus on how to adaptively sample the NN model using model uncertainty, which will alleviate the resampling stage of the algorithm. An important step in this work will be to characterize the computational cost and benchmark it against current state-of-the-art methods, as well as to perform numerical experiments on high-dimensional problems involving physical and computational data.

## Acknowledgements

This material is based upon work supported by the United States National Science Foundation under grant no. 1739551.

## References

1. Ferretti, F., Saltelli, A., Tarantola, S.: Trends in Sensitivity Analysis Practice in the Last Decades. *Science of the Total Environment* **568**, 666–670 (2016). <https://doi.org/10.1016/j.scitotenv.2016.02.133>
2. Iooss, B., Saltelli, A.: *Introduction to Sensitivity Analysis*. Springer International Publishing, Switzerland, 2015 (2015)
3. Sobol', I., Kucherekoand, S.: Sensitivity estimates for nonlinear mathematical models. *Mathematical Modelling and Computational Experiments* **1**, 407–414 (1993)

4. Sobol', I.: Global sensitivity indices for nonlinear mathematical models and their monte carlo estimates. *Mathematics and Computers in Simulation* **55**, 271–280 (2001)
5. Zhou, X., Lin, H.: Local Sensitivity Analysis. *Encyclopedia of GIS* pp. 1116–1119 (2017)
6. Homma, T., Saltelli, A.: Importance Measures in Global Sensitivity Analysis of Nonlinear Models. *Reliability Engineering and System Safety* **52**, 1–17 (1996)
7. Liu, Y.C., Nagawkar, J., Leifsson, L., Koziel, S., Pietrenko-Dabrowska, A.: Iterative global sensitivity analysis algorithm with neural network surrogate modeling. In: Paszynski M., Kranzlmüller D., Krzhizhanovskaya V.V., Dongarra J.J., Sloot P.M. (eds) *Computational Science – ICCS 2021*. *ICCS 2021. Lecture Notes in Computer Science*, vol 12745. Springer, Cham. (2021). [https://doi.org/10.1007/978-3-030-77970-2\\_23](https://doi.org/10.1007/978-3-030-77970-2_23)
8. McKay, M.D., Beckman, R.J., Conover, W.J.: A comparison of three methods for selecting values of input variables in the analysis of output from a computer code. *Technometrics* **21**(2), 239–245 (1979), <http://www.jstor.org/stable/1268522>
9. Goodfellow, I., Bengio, Y., Courville, A.: *Deep Learning*. The MIT Press, Cambridge, MA (2016)
10. Haykin, S.S.: *Neural networks and learning machines*. Pearson Education, Upper Saddle River, NJ, 3<sup>rd</sup> edn. (2009)
11. Schmidhuber, J.: Deep learning in neural networks: An overview. *Neural Networks* **61**, 85 – 117 (2015). <https://doi.org/10.1016/j.neunet.2014.09.003>
12. Gurralla, P., Chen, K., Song, J., Roberts, R.: Full wave modeling of ultrasonic NDE benchmark problems using Nystrom method. *Review of Progress in Quantitative Non-destructive Evaluation* **36**(1), 1–8 (2017)
13. Du, X., Leifsson, L., Meeker, W., Gurralla, P., Song, J., Roberts, R.: Efficient Model-Assisted Probability of Detection and Sensitivity Analysis for Ultrasonic Testing Simulations Using Stochastic Metamodeling. *Journal of Nondestructive Evaluation, Diagnostics and Prognostics of Engineering Systems* **2**(4): **041002**(4) (09 2019), <https://doi.org/10.1115/1.4044446>